# MICROWAVE DIELECTRIC MEASUREMENTS IN POTASSIUM DIHYDROGEN PHOSPHATE

by

Richard Ward Cole

# United States
# Naval Postgraduate School

# THESIS

MICROWAVE DIELECTRIC MEASUREMENTS IN

POTASSIUM DIHYDROGEN PHOSPHATE

by

Richard Ward Cole

June 1969

# Microwave Dielectric Measurements in Potassium Dihydrogen Phosphate

by

Richard Ward Cole
Lieutenant(junior grade), United States Navy
B.S., University of Rochester, 1968

Submitted in partial fulfillment of the
requirements for the degree of

MASTER OF SCIENCE IN PHYSICS

from the

NAVAL POSTGRADUATE SCHOOL
June 1969

ABSTRACT

This thesis describes the construction and operation of an X - band microwave system for measurement of the dielectric constant of ferroelectric materials, and also the construction of a broad band, coaxial sample holder. Preliminary measurements of the dielectric constant of potassium dihydrogen phosphate (KDP) at approximately 9.4 GHz show this to be above the dielectric relaxation frequency of this solid. Extensive measurements made to detect the coupled proton tunneling - soft mode in KDP show that the mode does not reach this low a frequency, which is attributed to the slight first order nature of the transition.

TABLE OF CONTENTS

LIST OF ILLUSTRATIONS

ACKNOWLEDGEMENT

The author wishes to express his great appreciation for the help, guidance, and patient instruction given him throughout the past year by Professor Gordon E. Schacher of the Naval Postgraduate School.

# I. INTRODUCTION AND THEORY

A ferroelectric material is one which has a spontaneous, reversible, electric polarization. Such a material is the electric analog of ferromagnetic materials: it has hysteresis and its polarization disappears above a transition temperature, $T_c$, where the material is in the normal paraelectric state. There are three sources of the polarization: atomic, lattice, and dipolar. Atomic polarization results from the distortion of the electron clouds of individual atoms. Lattice polarization results from the displacement of charged ions relative to one another and to their equilibrium sites. Dipolar polarization occurs when permanent molecular dipole moments are aligned. Below $T_c$, the electrostatic alligning forces which cause alignment of permanent dipoles or produce electronic or lattice dipole moments are stronger than the random thermal fluctuations, leading to a net dipole alignment. In the ferroelectric region, the spontaneous polarization, $P_s$, is a strong function of temperature, reaching saturation at $T = 0$ where all dipoles are aligned.

The dielectric constant of a ferroelectric crystal behaves anomalously. At a given frequency, the dielectric constant $\varepsilon(T)$ is a continuous function of the temperature, but it becomes extremely large ($\sim 10^4$) at $T = T_c$. The dielectric constant measures the response of a system to an electric field, and a large value of $\varepsilon$ near $T_c$ means that a small field yields a relatively large polarization. Near $T_c$, the electrostatic and thermal interactions are nearly equal, so that a small field would be expected to produce a large polarization. The dielectric peak is very useful in locating the transition temperature of a material.

Cochran's theory [Ref. 6] of ferroelectricity attempts to explain the behavior of the macroscopic dielectric constant in terms of the microscopic properties of a ferroelectric crystal. The description below applies to displacive ferroelectrics. Cochran considered the normal vibrational modes of a crystal and hypothesized that for one particular mode, at a certain temperature the short-range restoring forces and the long-range electrostatic interaction will almost cancel one another. The net restoring force would then be very small and the crystal would become unstable with respect to that particular mode. According to Cochran, this "ferroelectric mode" is the cause of the ferroelectric properties of the crystal. Because of the low restoring force, the characteristic frequency, $\nu_o$, of this mode is much lower than that of other modes. (i.e., The mode is "soft.") This model predicts $\nu_o$ to be temperature - dependent. The Lyddane - Sachs - Teller relation, [Ref. 9],

$$\frac{\omega_T^2}{\omega_L^2} = \frac{\varepsilon(\infty)}{\varepsilon(0)} ,$$

tells us that the static dielectric constant, $\varepsilon(0)$, becomes maximum when $\nu_o$ becomes minimum. Here $\omega_L$ and $\omega_T$ are the longitudinal and transverse frequencies, respectively. Cochran's theory shows that the temperature at which $\nu_o$ is minimum and $\varepsilon(0)$ is maximum occurs at the onset of spontaneous polarization. It is the $\vec{k} = 0$, transverse - optical mode which goes soft, because this infinite - wavelength mode is the one connected to the macroscopic polarization. (i.e., A $\vec{k} = 0$, transverse - optical mode is the one for which all positive charge centers move in one direction and all negative charge centers move in another.) At $T_c$, because of the smallness of the restoring force, new positions become energetically possible. These new positions result in net displacements of the positive and negative ion sublattices with respect to one another.

Hence we get the net spontaneous polarization below $T_c$ which is characteristic of ferroelectricity. Cochran's theory predicts that the new positions become stable at a predictable temperature, yielding a microscopic theory of ferroelectricity.

While the above analysis was developed to explain displacive ferroelectrics in general, this paper is concerned with only one ferroelectric, potassium dihydrogen phosphate, $KH_2PO_4$, (KDP). The transition temperature of KDP is $T_c = 121.8^\circ K \pm 0.1^\circ K$. Its crystal structure [Ref. 7] is tetragonal above $T_c$ and orthorhombic below $T_c$. In changing symmetry at $T_c$, the orthorhombic a- and b- axes are at $45^\circ$ to the tetragonal a- and b- axes, while the c- axis does not change direction and shows only a small change in lattice constant. The spontaneous polarization is along c. The KDP molecule itself consists of a $PO_4^{3-}$ tetrahedron (a $P^{5+}$ ion in the center of a tetrahedron, the corners of which are occupied by $O^{2-}$ ions) ionically bound to a $K^+$ ion. Each molecule also has two hydrogens associated with it. The natural place for these in the lattice should be in the position of hydrogen bonding, so each proton forms a modified hydrogen bond between oxygens of adjacent tetrahedra. This modified bond is longer than a normal hydrogen bond, and it has the energy configuration of a double potential well, with two possible positions for the proton corresponding to the minima of the two wells. Thus a proton can have two positions with respect to a given tetrahedron; in the "close" well or in the "far" well.

In the ferroelectric phase of KDP, the $K^+$ ions and the phosphate tetrahedra are displaced relative to one another along the c- or ferroelectric-axis. This net relative displacement of positive and negative charge centers yields a dipole moment of such a magnitude as to satisfactorily explain the observed magnitude of the saturated polarization

of KDP without any reference to the action of the hydrogen bonds. Certain large isotope effects were unexplained, however, until Blinc [Ref. 8] accounted for them with a model in which the proton is assumed to carry out a tunneling motion between the two minima of the potential along the modified hydrogen bond. As Kobayashi [Ref. 2] points out, the large displacements of the $K^{+}$ and $P^{5+}$ ions which accompany the protonic order - disorder transition in KDP suggest that the proton motion is strongly coupled to the $K\text{-}PO_4$ vibration along the c-axis. Hence the tunneling mode is closely coupled to the ferroelectric soft mode, and the frequency of this coupled mode goes to zero as the transition temperature is approached from above. This result is obtained from Cochran's theory [Ref. 6] as applied to the special case of KDP. In using Cochran's theory for this system, however, Kobayashi [Ref. 2] emphasizes that it is the proton ordering in the double potential well configuration of the hydrogen bonds that causes the frequency of the coupled mode to go to zero, unlike the case of displacive-type ferroelectrics such as barium titanate.

Cochran's theory predicts the observed peak in the dielectric constant of KDP at its transition temperature, but the theory does not specifically consider the coupled tunneling mode. Silverman [Ref. 9] takes this mode into account and predicts that, if an AC electric field is applied along the ferroelectric axis of KDP at temperatures slightly above the transition temperature, absorption of energy from the applied field will occur when the frequency of the field is equal to the proton tunneling frequency. Of course, the tunneling frequency is temperature dependent, because of the coupling to the soft mode. This energy absorption occurs because the tunneling mode is able to absorb energy resonantly at its characteristic frequency. Silverman indicates that

the tunneling frequency should be in the microwave region for temperatures about $0.1^{\circ}C$ from $T_c$. The occurrence of this resonance absorption should manifest itself in a greatly increased loss tangent for the material at the tunneling frequency. From the Kramers - Krönig dispersion relations, we see that a peak in the loss tangent should occur simultaneously with a decrease in the dielectric constant. Hence, if Silverman's theory is correct, a sharp dip should occur in the curve of dielectric constant versus frequency at constant temperature if this temperature is slightly above $T_c$. The frequency of such a dip would be the tunneling frequency of the hypothesized tunneling mode. Thus, Silverman's predictions can be illustrated on a theoretical graph of dielectric constant versus frequency at constant temperature similar to the one sketched in Figure 1. below.

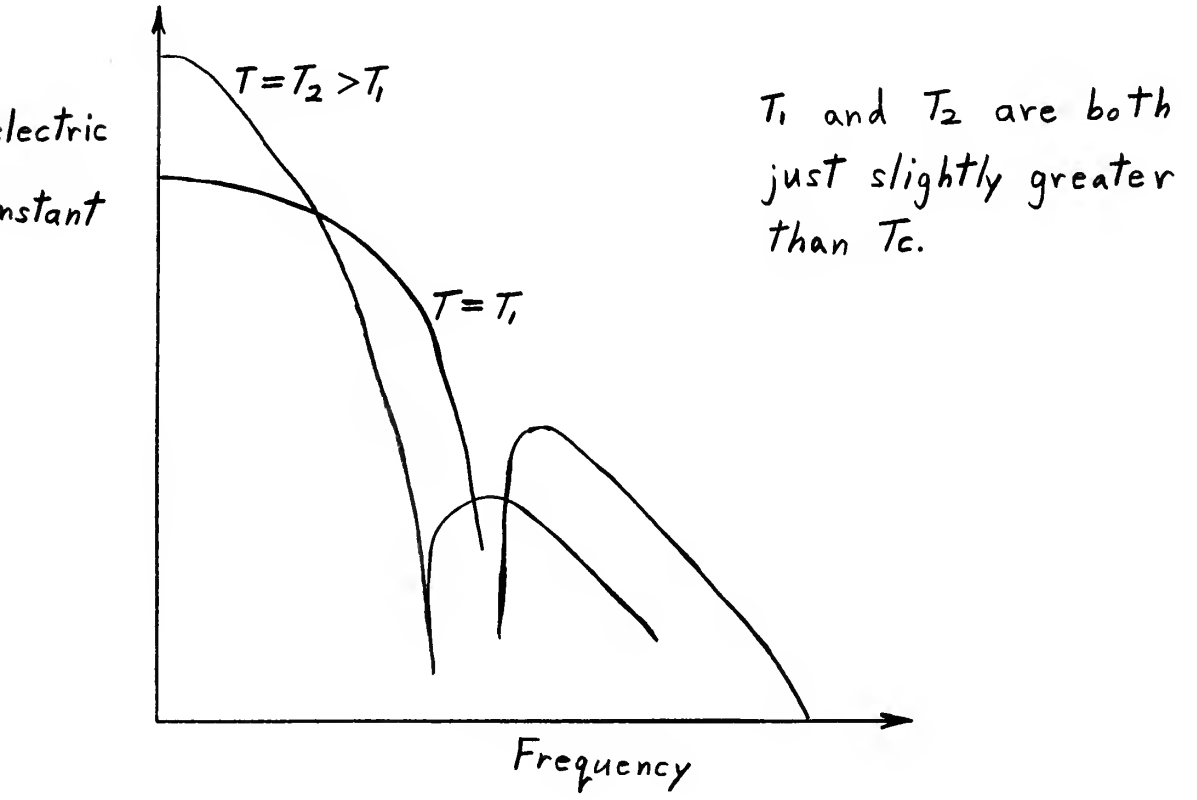


FIGURE 1. (Schematic)

However, Brillouin scattering results [Ref. 10] indicate that the soft mode never reaches zero frequency because of interference with the accoustic lattice vibrations. If this is the case, the tunneling mode will not reach as low a frequency as predicted by Silverman.

In this experiment, we are trying to test Silverman's theory by measuring the dielectric constant of KDP at $\sim$9 GHz and at very precisely controlled temperatures near $T_c$, and thus determine experimentally whether or not the resonant absorption predicted in Figure 1 occurs. The dielectric constant is determined by measuring the voltage standing wave ratios and shifts in the minima of the standing wave patterns in a coaxial line terminated by a KDP sample. From this data, we can calculate the values of dielectric constant vs. temperature needed to confirm or refute Silverman's prediction.

In Chapter II of this thesis, the microwave and thermal control equipment used for the measurements are described in detail. Chapter III outlines the sample preparation processes, while Chapter IV summarizes the calibration procedure and the calculation of the dielectric constants. Finally, Chapter V presents the experimental results and conclusions.

## II. EXPERIMENTAL EQUIPMENT

### A. MICROWAVE SYSTEM

The microwave circuit diagram is shown in Figure 2. Microwaves are generated in the system by an X-13 klystron, which is powered by a Varian V4500-10A E.P.R. control unit. The X-13 operates effectively from 9 to 12 GHz. Following the klystron in the circuit, we have an isolator, a frequency meter, and a 20 D.B. variable attenuator. Microwave power is measured with a Sperry Microline, model 31A1, average power meter and thermistor.

The next circuit element is a "magic T" modulator. One arm of the magic T is terminated by a matched load, and the other arm by a tunable crystal detector mount. The 1N415E crystal in this mount carries a 1000 cycle current which causes an alternating imbalance of the bridge formed by the magic T, the crystal being driven by an oscillator and biasing battery as in Figure 2. The net result is to superimpose a 1000 cycle amplitude modulation on our microwave signal so that a Hewlett-Packard, model 415BR, standing wave indicator can be used to measure VSWR. The oscillator level and the biasing voltage are adjusted to yield the best waveform for the modulation envelope.

Following the modulator, a 20 D.B. coupler and crystal detector monitor the signal for two purposes: to monitor the modulation envelope and to provide a signal for the E.P.R. console in order to tune the console. Next, an isolator is placed in the circuit to decouple the modulation and measurement portions of the system, since motion of the probe in the slotted line can change the balance of the magic T modulator. This isolator is then follwed by a waveguide-to-coax adaptor, a

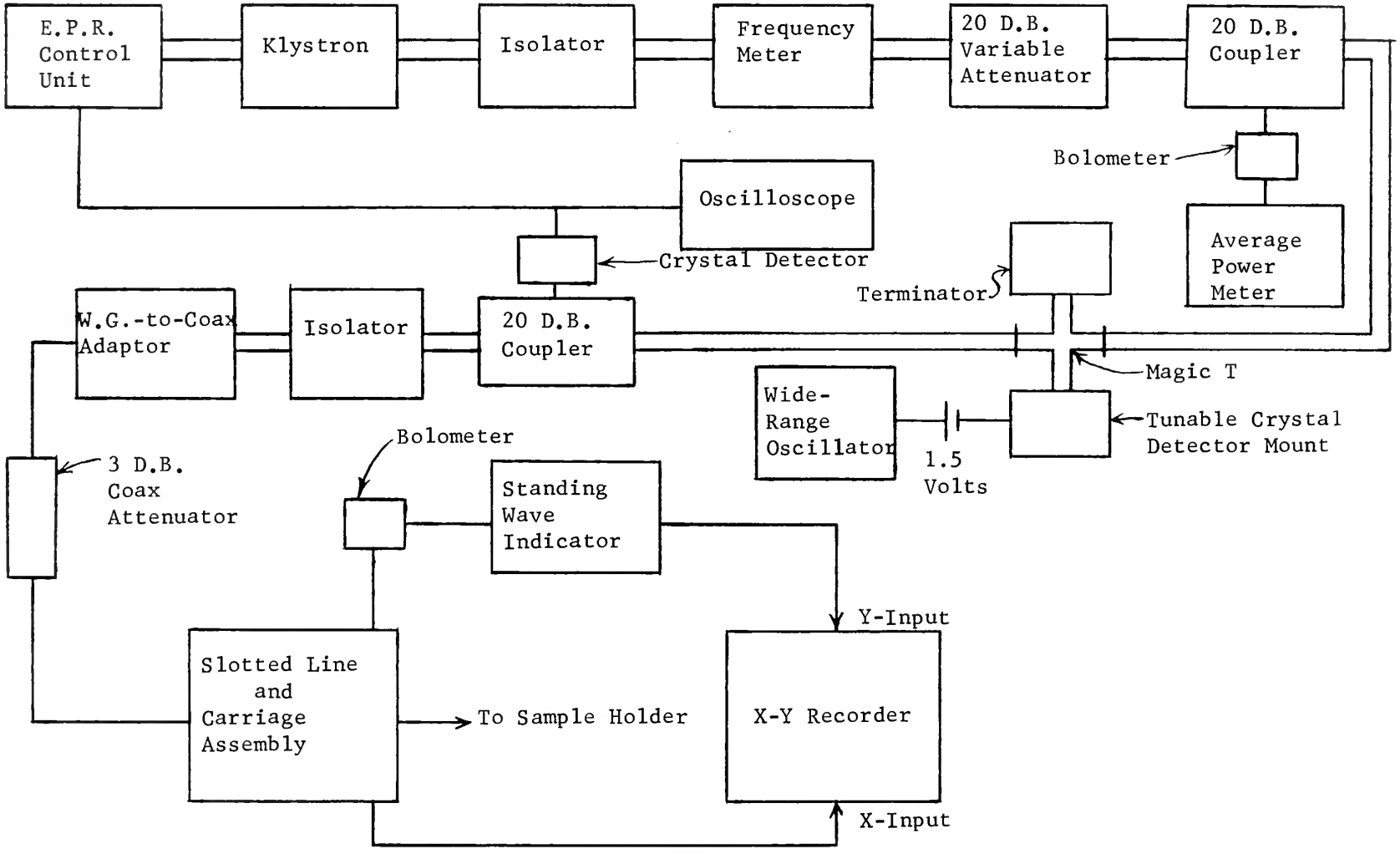


FIGURE 2. MICROWAVE SYSTEM

3 D.B. coaxial attenuator, and the slotted-line assembly. The 3 D.B. attenuator serves to reduce multiple reflections in the slotted line, which will distort the standing wave pattern.

The standing wave pattern in the coaxial slotted line is detected with a movable probe and bolometer in a tunable mount. The rider of a slide-wire rheostat is connected to the probe carriage to provide the x-axis drive for an x-y recorder. VSWR is determined from the standing wave indicator, whose recorder output is connected to the y-axis of the x-y recorder. Hence the x-y recorder gives a plot of the standing wave pattern in the slotted line, from which shifts in the standing wave minima can be measured very accurately.

This whole microwave system is peaked up so as to yield the best possible readings on the standing wave indicator. The frequency and shape of the modulation envelope are adjusted to give maximum sensitivity for the VSWR readings. This is done by varying the frequency of the crystal current in the modulator and by adjusting the length of the cavity in the tunable crystal detector mount. The cavity in the movable probe and the probe depth are also tuned for maximum sensitivity.

The coaxial sample holder is shown in Figure 3. It was built in such a way as to keep the sample stationary and in good electrical contact with both the end of the inner conductor and the flexible metal diaphragm which terminates the outer conductor. The sample is centered in the coaxial line by a teflon spacer. A pressure foot and spring hold the sample firmly in place to maintain the electrical contact. The sample holder is designed so as to insure a uniform electric field within the sample. The geometry of the end of the coaxial line, including the large area of the end of the inner conductor, produces a field at the sample site which is perpendicular to the two end faces, and which

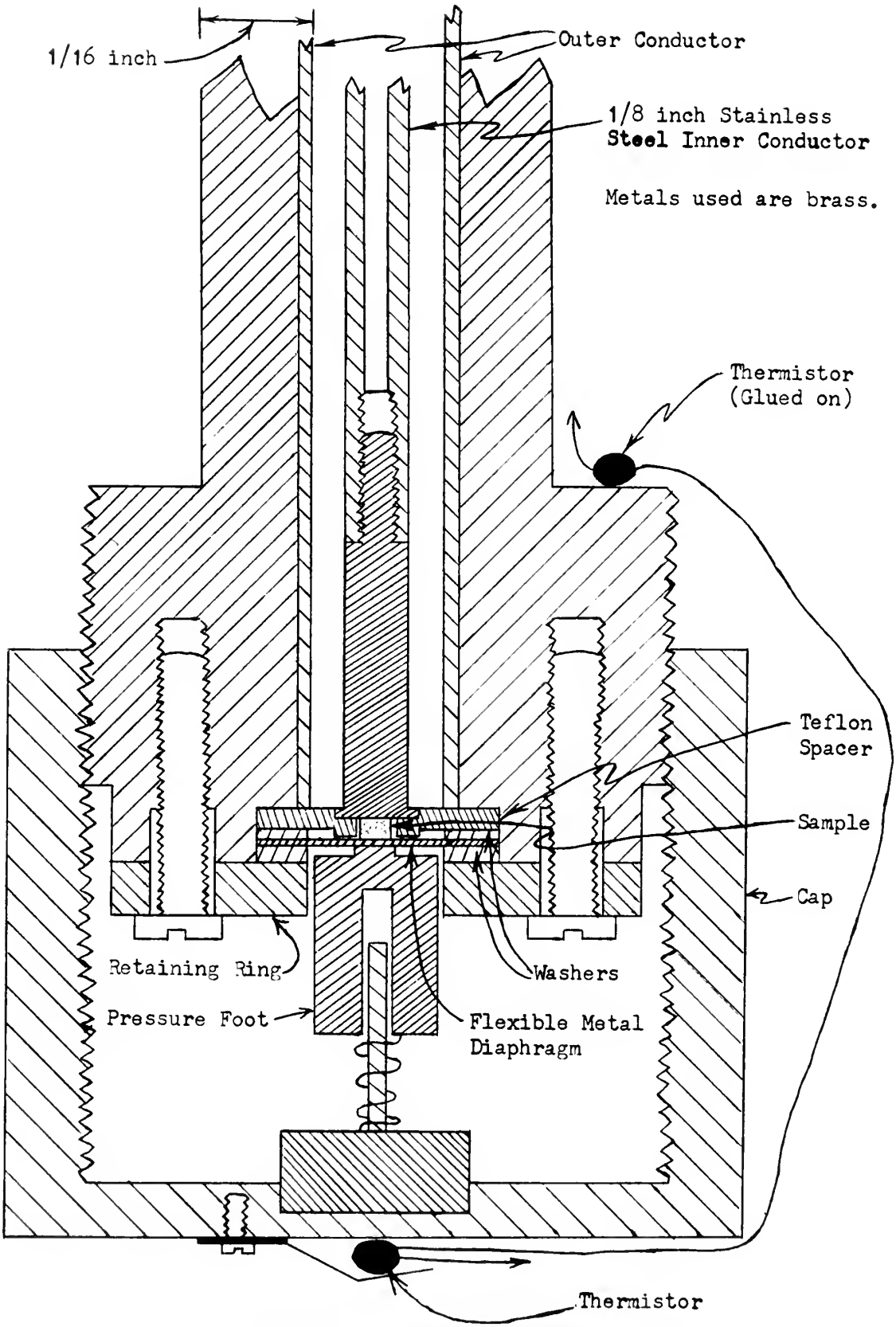


Figure 3. SAMPLE HOLDER

is nearly independent of the distance from the center axis over a large area. In addition, the high dielectric constant of the sample, which is cylindrical in shape, helps to reduce fringing effects. Thus in obtaining the sample dielectric constant from the measured VSWR, we are able to assume a uniform field.

The rigid coaxial line connecting the slotted line to the sample holder consists of two parts. The lower 11½ inches of the coaxial line is made of thinwall, stainless steel: the outer conductor having a ¼ inch inner diameter and the inner conductor having a 1/8 inch outer diameter. This part of the line has a 37 ohm impedence because the ratio of its diameters is 2:1. In order not to get reflections at the type-n connector (Figure IV), we need a line impedence of 50 ohms. Any other value will lead to an impedence mismatch with the type-n connector, and hence to reflections. For this reason, the upper 11 $^{11}/16$ inches of the coax consists of a tapered section for the outer conductor, the inner conductor remaining constant in diameter. The tapered section is made of copper, and is linearly tapered from 0.287 inches at its top to ¼ inch at the bottom. The bottom end is fitted smoothly to the stainless steel coax and the top end is attached to the type-n connector. The 0.287 inch diameter for the outer conductor at the top of the tapered section gives a diameter ratio of 2.3:1, which corresponds to a 50 ohm line impedence. Thus, the mismatch is eliminated and no reflections occur.

Details of the upper end of the cryostat support system are shown in Figure IV. Two thin - wall, stainless steel tubes lead from the vacuum can to the platform at the top of the rigid coax section. This platform is bolted down to a table. Besides providing mechanical support and stability for the system, these tubes also serve as conduits

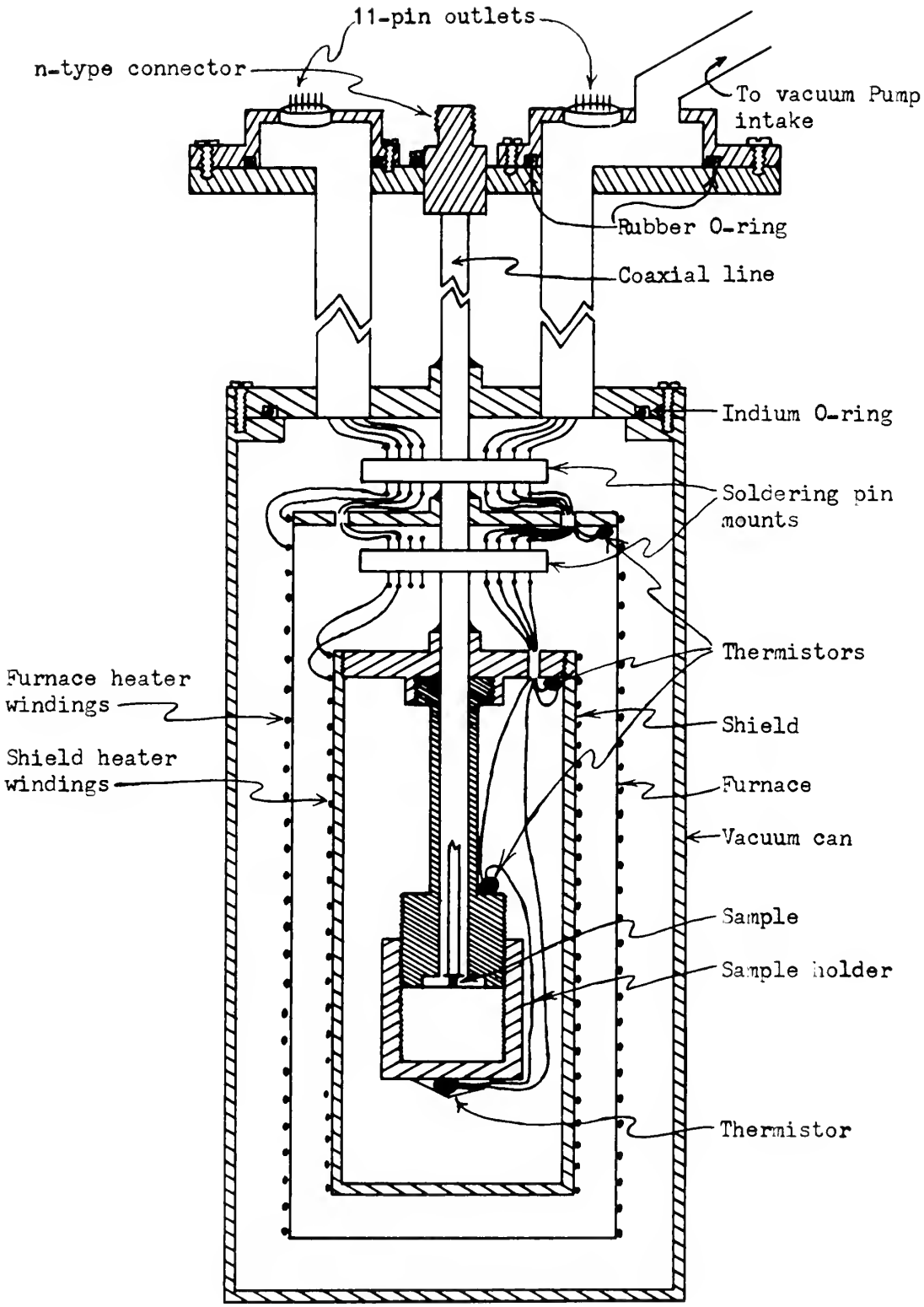


FIGURE IV. HOLDER SUPPORT + VACUUM CAN

along which the electrical wiring from the temperature-control thermistors and heaters are strung to two eleven - pin connectors on the platform. One of the tubes also leads to the pump system, and is used for evacuating the system.

B. THERMAL REGULATION SYSTEM

The temperature control electronics are drawn schematically in Figure 7, while the actual cryostat is sketched in Figure 4. A double shield system in a vacuum jacket is immersed in a bath of liquid nitrogen. The first stage of regulation, called the furnace, is a rough control used to elevate the temperature of the system to near $T_c$. It is an AC system, the circuit diagram of which appears in Figure 5. The furnace heater consists of about 40 feet of 11.54 $\Omega/ft.$ nichrome wire. The windings are evenly spaced over the surface of the furnace, including the end plates, in order to heat the interior uniformly.

The temperature detection devices used here, on the shield, and on the sample holder are low temperature thermistors. Their resistance is $7670 \pm 30$ ohms at $T_c$. Two are used in series on each can and on the sample holder to increase sensitivity. In the temperature region near $T_c$, the resistance of these thermistors varies with temperature as

$$\frac{dR}{dT} = .05R.$$

The second stage of temperature regulation, called the shield, consists of a DC Wheatstone bridge control system. The reference resistance for the bridge is provided by a Decabox DB62 standard resistance box in a temperature controlled chamber. The error signal from the bridge is proportional to the resistance difference between the shield thermistor and the reference resistance. This signal is fed to a Kiethley, model 153, microvolt-ammeter, which is used to monitor the

imbalance signal and as a DC amplifier. The output of the amplifier drives the control circuit shown in Figure 6. The shield heater is made up of about 20 feet of the same nichrome wire that was used in the furnace heater, wound in the same manner.

This whole system is evacuated to about 10 m.m. of mercury for thermal isolation. The sample holder screws directly to the shield, so the sample reaches thermal equilibrium at the same temperature as the shield, and the shield controller is used to regulate the sample temperature.

Sample temperatures are measured with an AC detection system, consisting of the thermistors, an AC Wheatstone bridge, reference resistance, and a lock - in detector. The lock - in detector output is plotted on a strip chart recorder. Temperature is determined by balancing the bridge with the reference resistance and reading this resistance.

This complete thermal control system allows us to maintain sample temperature constant to within about 0.2 millidegree, and to sense variations in this temperature of about the same magnitude.

The system is operated in the following way. The sample temperature is varied by changing the shield reference resistance. The shield temperature thus changes and the sample temperature slowly comes to equilibrium with the shield. The sample temperature is monitored on the recorder so one can determine when thermal equilibrium is reached.

ALL sample temperatures in this experiment are measured assuming $T_c = 121.8^{\circ}K$. A flat plate of KDP, with leads silver-painted to both faces is taped to the sample holder. A capacitance bridge is used to measure the capacitance of the KDP plate as a function of temperature. Since the capacitance is proportional to the static dielectric constant,

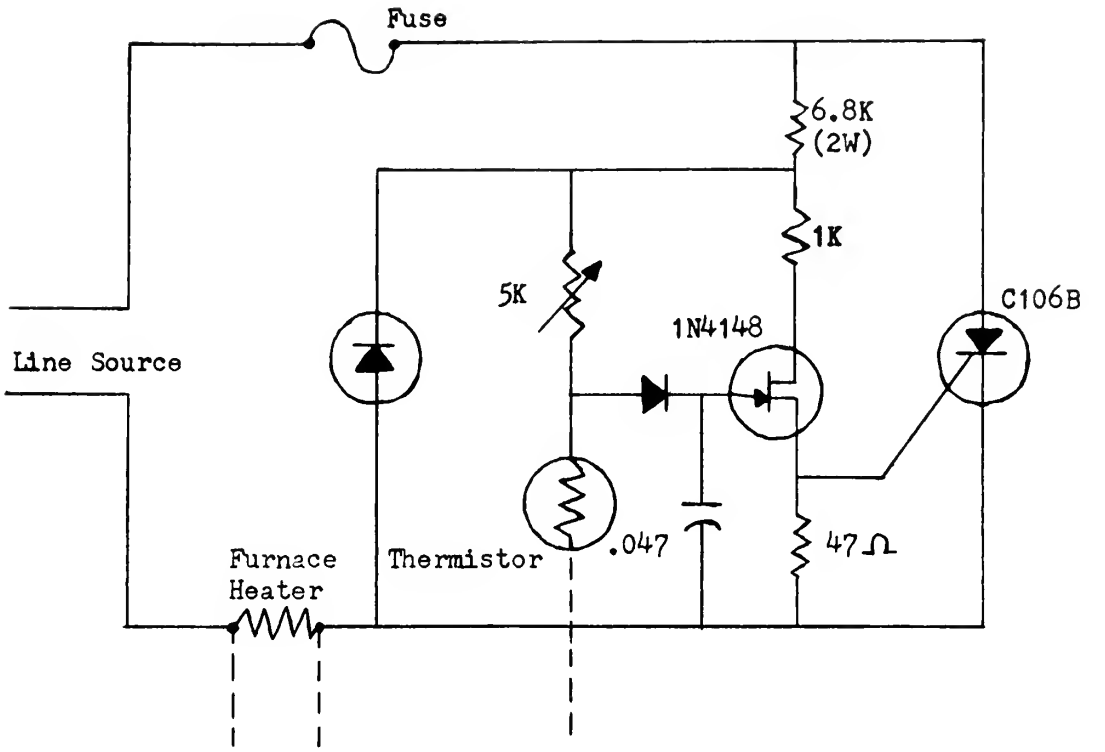


FIGURE 5. ROUGH TEMPERATURE CONTROLLER

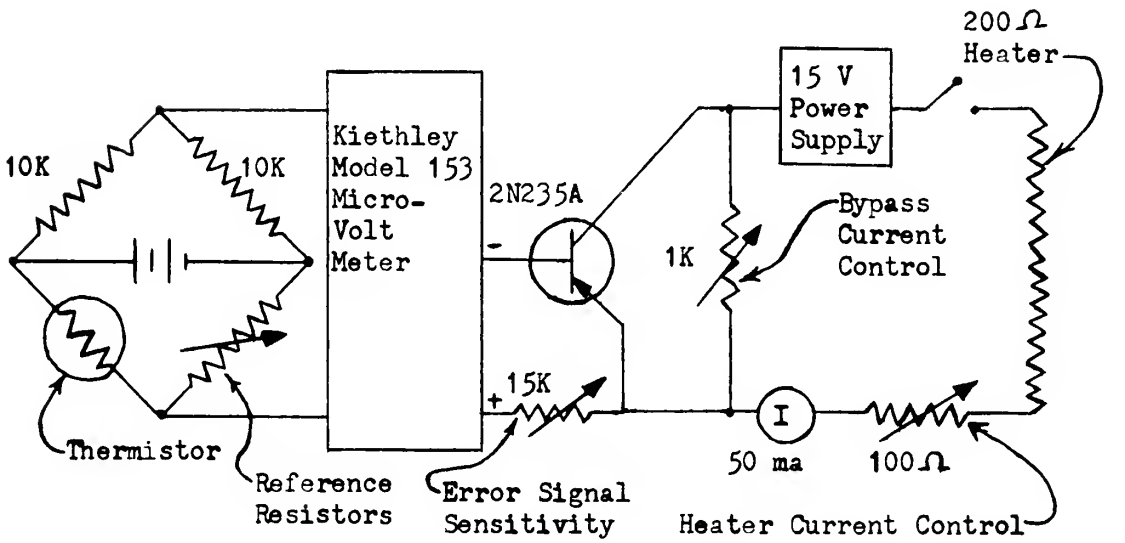


FIGURE 6. SHIELD HEATER CONTROL CIRCUIT

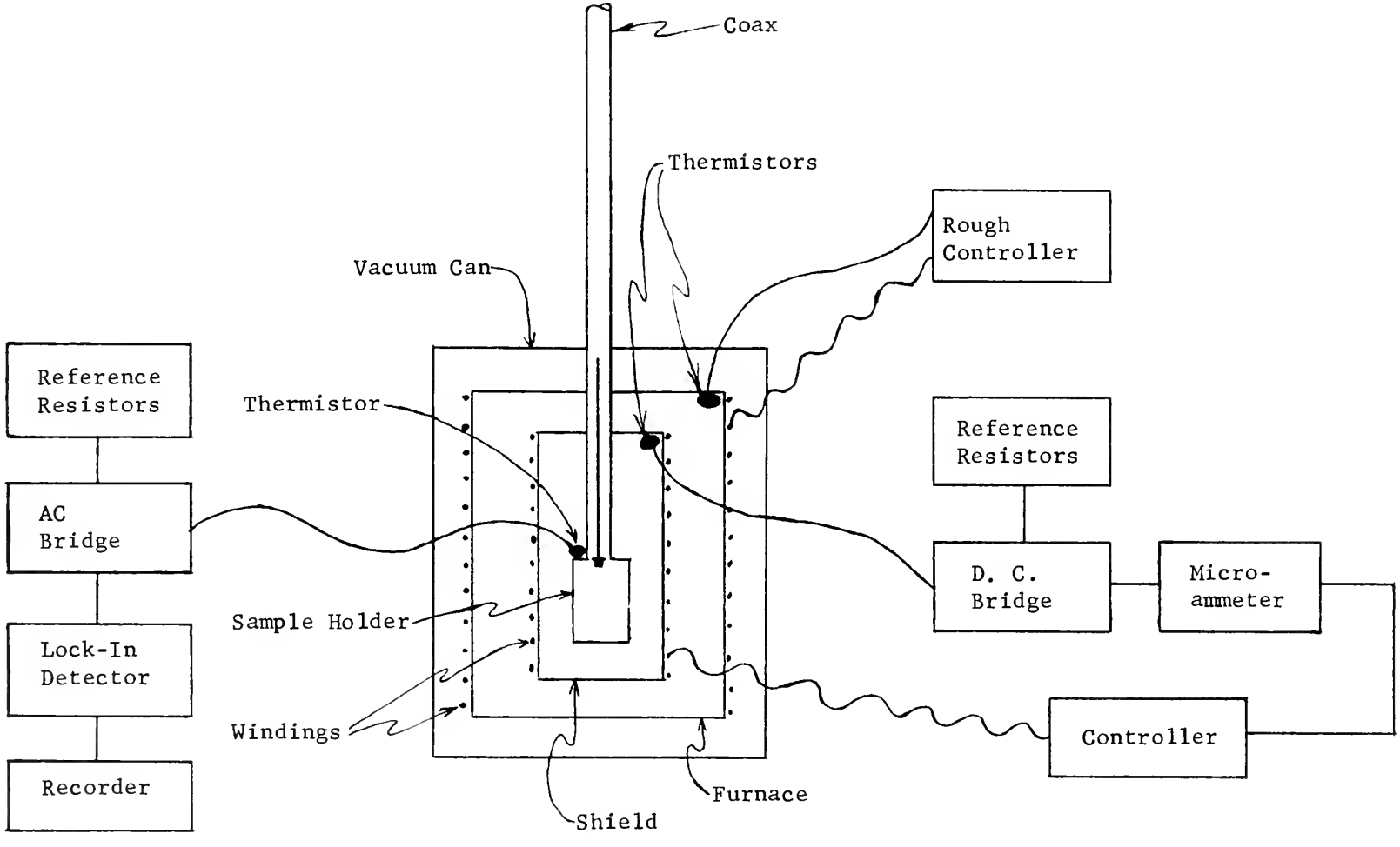


FIGURE 7. TEMPERATURE CONTROL SYSTEM

it has a sharp peak at the transition temperature. The thermistor resistance at which this peak is observed corresponds to the transition temperature $T_c$. This calibrates the thermistor. Then, using the known relation

$$\frac{1}{R}\frac{dR}{dT} = 0.05,$$

temperature variaions from $T_c$ can be measured in ohms of thermistor resistance.

## III. SAMPLE PREPARATION

For calibration purposes, samples of NaCl, LiF, teflon and brass were prepared, along with the samples of TGS and KDP required for preliminary and final measurements, respectively. These samples had to be in the shape of a right circular cylinder, with height between 35 and 50 mils and cross - sectional diameter between 60 and 75 mils. For both KDP and TGS, the ferroelectric axis had to be along the symmetry axis of the cylinder.

The brass sample was made on a metal lathe. A brass rod was inserted in the lathe and about half a centimeter of its length was turned down to the proper diameter and cut off in the usual manner. The teflon sample was prepared from a teflon rod in much the same manner as was the brass sample. The end of the rod was turned down to the correct diameter. In this case, however, some difficulty was experienced because the teflon bent easily on the lathe when its diameter became small. This was overcome by making the turned - down section as short as possible. A razor blade was then used to cut the correct sample length from the rod.

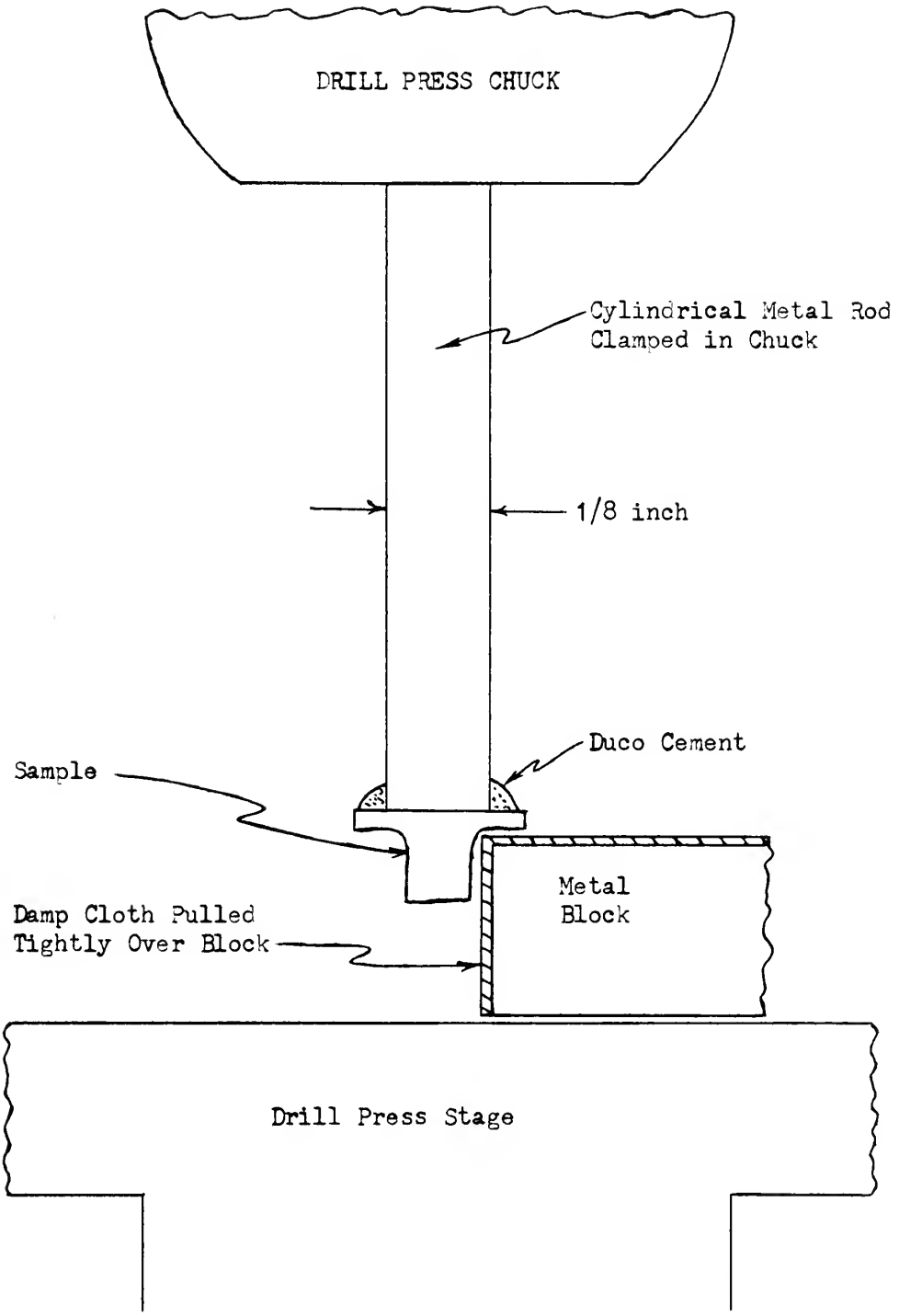


FIGURE 8. SAMPLE GRINDING ON JEWELER'S DRILL PRESS

The NaCl, LiF, TGS and KDP samples were prepared on the jeweler's drill press pictured in Figure 8. A metal rod about 1/8 inch in diameter was inserted in the drill press chuck and the sample piece to be ground was cemented to the base of the rod with Duco glue. The pieces used were roughly cylindrical in shape, with diameters slightly larger than that of the rod on which they were mounted. The heights of the pieces were somewhat greater than the height required for the finished samples. In the cases of KDP and TGS, the pieces had to be cleaved or cut so that their ferroelectric axes were parallel to the cylinder axes of the samples. NaCl, TGS and KDP are all water-soluble. Only LiF is insoluble in water. Hence, a wet string-saw was used to cut the first three types, while LiF was cut with a jeweler's saw.

The three soluble crystals were ground down on the drill press by water-polishing. A wet cloth was pulled tightly over the edge of a rectangular metal block set on the drill press stage as shown in the figure. The drill was rotated so that the cylindrical edge of the sample touched the cloth and the moisture in the cloth dissolved away the side of the cylinder, uniformly decreasing its diameter. As shown in the drawing, a small "hat" of sample material was left above the block so that moisture from the polishing cloth didn't dissolve the top of the sample away from the glue, causing it to fall off. When the sample diameter had been ground down to the correct size, the sample was removed from the press and soaked in acetone to remove the remnants of Duco glue. The bases of the cylinder were then polished down by rubbing them on the flat surface of a damp cloth spread on a table until the "hat" was gone and the cylinder was the right height for use as a sample.

The LiF sample, since it was not soluble, had to be ground down with sandpaper instead of water. A small strip of fine sandpaper was held against the side of the sample as it spun on the drill press, thus wearing away the cylindrical surface evenly. It was found that, if the sandpaper was not too coarse and was held loosely enough, the crystal was ground down smoothly and quickly. After the proper diameter had been reached, the bases of the cylinder were ground down with sandpaper until the LiF cylinder was the correct height to act as a sample.

All of the samples except brass were silver-painted on their two bases so they would establish good electrical contact in the sample holder.

## IV. CALIBRATION AND DATA REDUCTION[1]

The data obtained directly from our measurements are in the form of VSWR readings from the standing wave indicator and shifts in standing wave minima from the x-y recorder, as previously described. From each of these sets of readings, we must get a value for the dielectric constant of the sample.

A VSWR measurement and the shift in position of the minimum can be used to calculate a value for the impedence Z at the slotted line from the formula:

$$Z_m = \frac{1 - |\rho|^2 - 2i|\rho|\sin(4\pi\Delta)}{\{1 + |\rho|\cos(4\pi\Delta)\}^2 + \{|\rho|\sin(4\pi\Delta)\}^2}, \qquad (1.)$$

$$\text{where} \quad |\rho| = \frac{VSWR - 1}{VSWR + 1}. \qquad (2.)$$

Here $\Delta$ is the fractional wavelength shift in the position of the minimum from its position when a brass calibration sample is used in the sample holder as a short between inner and outer coaxial conductors. $\Delta$ is defined to be positive when the minimum shifts toward the microwave source. The impedence $Z_m$ determined here is the impedence of the entire system, from the probe in the slotted line to the sample. We thus measure the impedence of part of the slotted line, a section of coax, the sample holder, and the sample. The value found will be

---

[1]This section depends heavily on the material in Chapter 3 of Ref. 1 and is presented here for completeness.

strongly affected by reflections occurring at the sample boundary, the base of the sample holder, the junction to the slotted line, and in the slotted line itself. It is necessary to determine how the impedence of the sample, which is the value desired, is related to the impedence $Z_m$ measured at the slotted line.

Following Reference 1, this is done by considering the part of our system from sample holder to slotted line probe to be a two-port microwave circuit, the input port being an arbitrary cross-sectional plane in the slotted line. The TEM coaxial mode is the only mode present at this port. The output port is the cylindrical surface of the sample. Although modes other than the dominant TEM mode may be present in this cricuit, it can be shown theoretically that they do not couple to the input mode, and hence will not be considered. The analysis which follows will be carried out in terms of admittances, where the admittance is defined as the reciprocal of the impedance. It can be shown [Ref. 4] that in any multiport microwave circuit, the admittances of all modes present at all of the ports are bilinearly related. We will now determine the bilinear relationship between the output admittance of the one propagating mode and the input admittance measured in the slotted line. We will also show that the coefficients in this bilinear expression can be experimentally measured.

Denote the current and voltage measured in the slotted line by $I_m$ and $V_m$, respectively. Then $Y_m = I_m/V_m$ is the admittance measured at this plane. The corresponding quantities at the cylindrical edge of the sample are denoted by $I_o$, $V_o$, $Y_o$. The two sets of values can be related bilinearly by the matrix expression

$$\begin{pmatrix} V_m \\ I_m \end{pmatrix} = \begin{pmatrix} A & B \\ C & D \end{pmatrix} \begin{pmatrix} V_o \\ I_o \end{pmatrix},$$

with

$$AB - CD = 1. \tag{3.}$$

Then $Y_m$ and $Y_o$ will be related, in the most general way, by

$$Y_m = \frac{C + D\,Y_o}{A + B\,Y_o}. \tag{4.}$$

We may now replace the continuous two-port microwave circuit with distinct elements for calculational purposes. There are an infinite number of possible imaginary circuits which could be used to give the same relationship between $Y_m$ and $Y_o$, but still following the development of Ref. 1, we use the following:

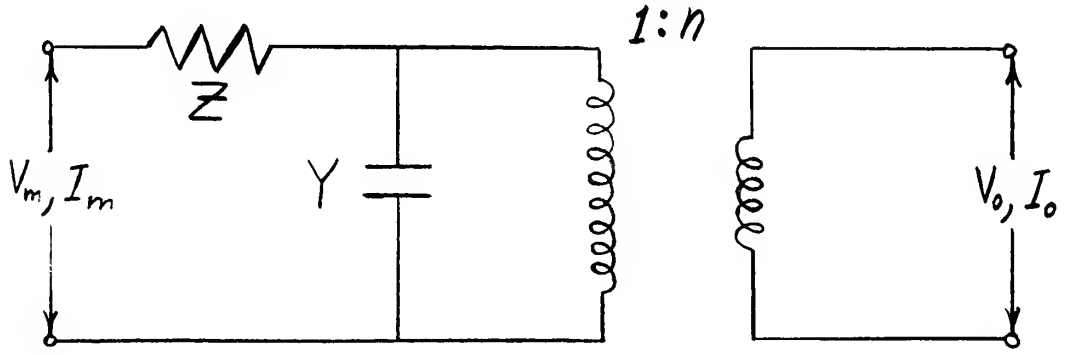


The bilinear relation for the voltage and currents now becomes

$$\begin{pmatrix} V_m \\ I_m \end{pmatrix} = \begin{pmatrix} 1 & Z \\ 0 & 1 \end{pmatrix}\begin{pmatrix} 1 & 0 \\ Y & 1 \end{pmatrix}\begin{pmatrix} 1/n & 0 \\ 0 & n \end{pmatrix}\begin{pmatrix} V_o \\ I_o \end{pmatrix}$$

$$= \begin{pmatrix} \dfrac{1+YZ}{n} & nZ \\ \dfrac{Y}{n} & n \end{pmatrix}\begin{pmatrix} V_o \\ I_o \end{pmatrix},$$

so that $Y_m$ is given by

$$Y_m = \frac{Y + n^2 Y_0}{1 + YZ + n^2 Z Y_0} . \qquad (5.)$$

This equation gives us the measured admittance as a function of the true sample admittance only, if we can experimentally determine the adjustable parameters Y, $n^2$, Z. These must be chosen so as to make Eq. (5) identical to Eqs. (3) and (4). Since the circuit considered here is imaginary and its elements need not correspond to true resistors, capacitors and transformers, it must be assumed that Y, $n^2$ and Z all have complex values and unknown frequency dependences. We now calibrate the system at each frequency to find Y, $n^2$ and Z, thus giving the unknown $Y_0$ in terms of the measured $Y_m$ in Eq. (5).

The calibration procedure is as follows. A brass cylinder the same size as the samples is placed in the sample holder and its impedence is measured with the slotted line. For the brass, we assume $Y_0 = \infty$ so that $Y_m = 1/Z$ from Eq. (5). The input port in this circuit has been defined to be a cross-sectional plane in the slotted line, but we have not specified the location of this plane as yet. We now define it to be one of the minima of the standing wave pattern for this brass sample so as to make Z a real number. The parameter Z is thus obtained from the measured $Y_m$ in this case.

We can now obtain the real part of Y by measuring the admittance of the empty sampe holder, in which case we may assume $Y_0 = 0$. This gives us

$$Y_m = \frac{Y}{1 + YZ}$$

from Eq. (5). In general we have $|YZ| << 1$, so that the real part of Y equals the real part of $Y_m$ when the sample holder is empty.

The approximation $Y_o = 0$ for the empty sample holder is not, however, adequate for the determination of the imaginary part of Y. For this, we must also measure $Y_m$ for a sample of known dielectric constant. In addition to the imaginary part of Y, these measurements will also give us the real part of $n^2$. It can be shown by energy conservation that $IM(n^2) << Re(n^2)$, so we may assume $Im(n^2) = 0$ for this problem. We now anticipate the results that $Re(n^2) < 1$ and $Im(Y) << 1$, and use the fact that $Z \approx 1$ to find that Eq. (5) simplifies to

$$Y_m \approx Y + n^2 Y_o$$

with these approximations. Several samples with known, but different, dielectric constants were used in this procedure to increase the accuracy of the calibration and to improve the final value obtained for $n^2$.

From basic electrodynamics, we know that when a dielectric of capacitance C is placed in an AC electric field of angular frequency $\omega$, the imaginary part of the sample admittance is given by the equation [Ref. 4]

$$Im(Y_o) = \omega C. \qquad (6)$$

Our samples are cylindrical in shape. For a given sample of dielectric constant $\varepsilon$, call its height D and its cross-sectional area $A = \frac{1}{4}\pi d^2$, where d is the sample diameter. During the measurements, this sample is situated between the end plate of the inner conductor of the coax and the diaphragm across the end of the outer conductor, so the sample is effectively between the plates of a parallel plate capacitor. Again from elementary theory, we find that its capacitance in this

configuration is given by $C = \varepsilon \frac{A}{D}$, where fringing effects have been ignored because the sample diameter is considerably less than the diameter of either plate, and also because $\varepsilon$ is high for the samples in question. Putting this value for the capacitance into Eq. (6), we get

$$Im\,(Y_o) = \omega \varepsilon \frac{A}{D}. \qquad (7.)$$

The sample dimensions A and D can be measured with a micrometer. We know the frequency $\omega$ of our microwaves. Hence, Eq. (7) gives us $Im(Y_o)$ for each of our samples of known $\varepsilon$.

After calculating $Im(Y_m)$ from Eqs. (1) and (2) using measured values of VSWR and $\Delta$ for each of our calibration samples, and calculating $Im(Y_o)$ from Eq. (7) for these same samples, we then plot $Im(Y_m)$ versus $Im(Y_o)$. The intercept and slope of this plot give Im(Y) and $Re(n^2)$, respectively.

The calibration samples used in this procedure were NaCl, LiF and teflon. Von Hippel [Ref. 5] gives the following dielectric constants for these substances in the pertinent frequency range ($\sim 10^{10}$ c.p.s.):

| | | | |
|---|---|---|---|
| NaCl | $\varepsilon$ | = | 5.90, |
| LiF | $\varepsilon$ | = | 9.00, |
| Teflon | $\varepsilon$ | = | 2.08. |

These values were taken as standard for the calibration. The preparation of these calibration samples, as well as the brass sample and the KDP samples, is described in Chapter III. The technique for measuring $Y_m$ and the equipment used are described in Chapter II. The results obtained for the adjustable parameters Z, Y, $n^2$ are listed in Chapter V.

With these results, Eq. (5) now gives $Y_o$ as a function only of $Y_m$, and our system is properly calibrated to give the actual admittance $Y_o$ of a KDP sample from the value $Y_m$ measured at the slotted line. Now invert Eq. (7) to get

$$\varepsilon = \frac{D\ Im(Y_o)}{\omega A} . \tag{8.}$$

Using the value of $Y_o$ just obtained, this equation will give us the dielectric constant of our KDP sample as a function of frequency, as desired.

The computer program used to calculate these dielectric constants in the manner described here is printed out in the appendix.

## V. RESULTS AND CONCLUSIONS

The calibration parameters Y, Z, $n^2$ were obtained in the manner described in Chapter IV. The calibration was performed using microwaves in the frequency range $(9.375 \pm 0.004) \times 10^9$ Ghz., as was the complete set of KDP measurements. This frequency was selected to give the greatest power output from our klystron. The following values were found for the parameters:

$$Y = 1.85 - 6.0i,$$

$$Z = 0.417,$$

$$n^2 = +\ 5.25 \times 10^{-11}.$$

The physical dimensions of the samples used are listed in the table below.

SAMPLE DIMENSIONS (in centimeters)

| Sample | D = height | d = diameter |
|---|---|---|
| NaCl | .129 | .140 |

| Sample | D = height | d = diameter |
|---|---|---|
| Teflon | .150 | .137 |
| LiF | .138 | .142 |
| Brass | .152 | .136 |
| KDP | .135 | .139 |

In all, about 130 valid data points were taken for KDP from room temperature to liquid nitrogen temperature. Of these, about 90 were within one degree Centigrade above or below $T_c$, with the greatest concentration slightly above $T_c$, where the tunneling resonance was expected to occur. The data points near $T_c$ were taken by changing the sample temperature in about 10 millidegree steps. Several VSWR measurements were taken while thermal equilibrium was being achieved, so that readings were obtained in approximately one millidegree steps. It takes about one half hour for the sample and holder to come to equilibrium, so the sample temperature was not changing to any appreciable degree while a measurement was being made. The data points which were not taken near $T_c$ were taken at varying temperature intervals, the intervals being wider the further the sample was from $T_c$ .

It would have been most convenient for detecting the tunneling mode if the VSWR minimum position could have been monitored continuously. However, absorption of microwave energy by the sample and sample holder raises the temperature when measurements are being made, making continuous readings impossible. When measurements are made by turning on microwave power only for the time needed to take the readings, no rise in temperature is detectable.

The full range of dielectric constant data shows little, if any, increase in the dielectric constant near $T_c$ . This indicates that at X - Band frequencies we are beyond the dielectric relaxation frequency in KDP.

The measurements just above $T_c$ do not show any evidence of resonance absorption by a tunneling mode. The VSWR measurements were accurate to about 20% and, as indicated above, measurements were not made continuously but in about one millidegree steps. Even so, a resonant absorption of the type predicted by Silverman should be observed if present. The most probable conclusion is that the coupled tunneling - soft mode never reaches this low a frequency due to the slight first order nature of the transition [Ref. 11] . This is in agreement with the Brillouin scattering results [Ref. 10] mentioned in Chapter I.

```
LEVEL  1, MOD 3              MAIN                DATE = 69156          07/02/56

C       HIGH FREQUENCY DIELECTRIC CONSTANT CALCULATION
C       VSWR = VOLTAGE STANDING WAVE RATIO
C       DELTA = FRACTIONAL SHIFTS IN MINIMA FROM BRASS MINIMA
C       DEL = 4 * PI * DELTA
C       YMR = REAL PART OF MEASURED ADMITTANCE
C       YMI = IMAGINARY PART OF MEASURED ADMITTANCE
C       YSI = IMAGINARY PART OF SAMPLE ADMITTANCE
C       F = FREQUENCY IN CPS
C       D = SAMPLE DIAMETER
C       R = SAMPLE HEIGHT
C       Z, SON, YR, YI = CALIBRATION PARAMETERS
C       EPS = SAMPLE DIELECTRIC CONSTANT
C       I = NUMBERING INDEX FOR DATA POINTS
        REAL X,Y,VSWR(100),DELTA(100),RHO(100),DEL(100),YMR(100),YMI(100),
       17,SON,YR,YI,D,R,F(100),YSI(100),EPS(100)
        INTEGER I, M
        DEN1(X,Y) = 1. + X * COS(Y)
        DEN2(X,Y) = X * SIN(Y)
        READ(5,1) M, Z, SON, YR, YI, D, R
      1 FORMAT(I3,F10.0,F15.7,4F10.0)
        PRINT 100
    100 FORMAT(2X,'I     VSWR      DELTA           F                    EPS
       1',//)
      4 DO 25 I = 1, 100
        READ(5,2) VSWR(I), DELTA(I), F(I)
      2 FORMAT(2F10.0,E15.4)
        RHO(I)=(VSWR(I)-1.)/(VSWR(I)+1.)
        DEL(I) = 4.*3.14159*DELTA(I)
        YMR(I)=(DEN1(RHO(I),DEL(I))**2+DEN2(RHO(I),DEL(I))**2)*(1.-RHO(I)*
       1*2)/((1.-RHO(I)**2)**2+(2.*DEN2(RHO(I),DEL(I))**2))
        YMI(I)=(DEN1(RHO(I),DEL(I))**2+DEN2(RHO(I),DEL(I))**2)*(2.*DEN2(
       1RHO(I),DEL(I)))/((1.-RHO(I)**2)**2+(2.*DEN2(RHO(I),DEL(I))**2))
        YSI(I)=(Z*YMI(I)*(YMR(I)+Z*YR*YMR(I)-Z*YI*YMI(I)-YR) + (1.-Z*YMR(I
       1))*(YMI(I)+Z*YI*YMR(I)+Z*YR*YMI(I)-YI))/(SON*(1.-Z*YMR(I))**2+SON*
       1(Z*YMI(I))**2)
        EPS(I)=(2.*YSI(I)*R)/(3.14159**2*F(I)*D**2)
        PRINT 101,I,VSWR(I),DELTA(I),F(I),EPS(I)
    101 FORMAT(1X,I3,3X,F7.3,3X,E6.4,3X,E15.4,3X,E15.7,/)
        IF(I .GE. M) GOTO 26
     25 CONTINUE
     26 STOP
        END
```

LIST OF REFERENCES


1. Sandy, Frank, "Dielectric Dispersion in Ferroelectric Rochelle Salt," Air Force Cambridge Research Laboratories, AFCRL - 65 - 250, 1965.

2. Kobayshi, Kenji K., "Dynamical Theory of the Phase Transition in $KH_2PO_4$ - Type Ferroelectric Crystals," J. Phys. Soc. Japan 24, 3, 1968.

3. Silverman, B. D., "Frequency - Dependent Dielectric Constant of $KH_2PO_4$," Phys. Rev. Letters 20, 9, 1968.

4. Montgomery, G. C., Dicke, R. H., Purcell, E. M., "Principles of Microwave Circuits," Chapter 5, McGraw - Hill, 1948.

5. Von Hippel, A., "Dielectric Materials and Applications," Chapter 5, John Wiley and Sons, 1954.

6. Cochran, W., "Advances in Physics" ed. N. F. Mott, Taylor and Francis, Ltd., London, 1961, Vol. 10, p. 401.

7. Fatuzo, E., W. J. Mertz, "Ferroelectricity," John Wiley and Sons, 1967.

8. Blinc, R., J. Phys. Chem. Solids 13, 204, 1960.

9. Kittel, C., "Introduction to Solid State Physics," Third Ed., John Wiley and Sons, 1967.

10. Brody, Edward M and Cummins, Herman Z., "Brillouin Scattering Study of the Ferroelectric Transition in KDP," to be published.

11. Reese, W., "Studies of Phase Transitions in Order - Disorder Ferroelectrics III: The Phase Transition in $KH_2PO_4$ and a Comparison with $KD_2PO_4$ ." to be published in Phys. Rev., 10 May 1969.

INITIAL DISTRIBUTION LIST

| | | No. Copies |
|---|---|---|
| 1. | Defense Documentation Center<br>Cameron Station<br>Alexandria, Virginia 22314 | 20 |
| 2. | Library, Code 0212<br>Naval Postgraduate School<br>Monterey, California 93940 | 2 |
| 3. | Professor Gordon E. Schacher<br>Department of Physics<br>Naval Postgraduate School<br>Monterey, California 93940 | 1 |
| 4. | LTJG Richard W. Cole<br>24 Greenhill Terrace<br>West Seneca, New York 14224 | 1 |
| 5. | Commander, Naval Ordnance<br>Systems Command Hqs.<br>Department of the Navy<br>Washington, D. C. 20360 | 1 |

Security Classification

# DOCUMENT CONTROL DATA - R & D

*(Security classification of title, body of abstract and indexing annotation must be entered when the overall report is classified)*

| 1. ORIGINATING ACTIVITY (Corporate author) | 2a. REPORT SECURITY CLASSIFICATION |
|---|---|
| Naval Postgraduate School<br>Monterey, California 93940 | Unclassified |
| | 2b. GROUP |

3. REPORT TITLE

Microwave Dielectric Measurements in Potassium Dihydrogen Phosphate

4. DESCRIPTIVE NOTES (Type of report and, inclusive dates)

Master's Thesis; June 1969

5. AUTHOR(S) (First name, middle initial, last name)

Richard Ward Cole

| 6. REPORT DATE | 7a. TOTAL NO. OF PAGES | 7b. NO. OF REFS |
|---|---|---|
| June 1969 | 39 | 11 |

| 8a. CONTRACT OR GRANT NO. | 9a. ORIGINATOR'S REPORT NUMBER(S) |
|---|---|
| b. PROJECT NO. | |
| c. | 9b. OTHER REPORT NO(S) (Any other numbers that may be assigned this report) |
| d. | |

10. DISTRIBUTION STATEMENT

Distribution of this document is unlimited.

| 11. SUPPLEMENTARY NOTES | 12. SPONSORING MILITARY ACTIVITY |
|---|---|
| | Naval Postgraduate School<br>Monterey, California 93940 |

13. ABSTRACT

This thesis describes the construction and operation of an X - band microwave system for measurement of the dielectric constant of ferroelectric materials, and also the construction of a broad band, coaxial sample holder. Preliminary measurements of the dielectric constant of potassium dihydrogen phosphate (KDP) at approximately 9.4 Ghz show this to be above the dielectric relaxation frequency of this solid. Extensive measurements made to detect the coupled proton tunneling - soft mode in KDP show that the mode does not reach this low a frequency, which is attributed to the slight first order nature of the transition.

DD FORM 1 NOV 65 1473 (PAGE 1)

S/N 0101-807-6811

Security Classification

A-31408

| 14 KEY WORDS | LINK A | | LINK B | | LINK C | |
|---|---|---|---|---|---|---|
| | ROLE | WT | ROLE | WT | ROLE | WT |
| Ferroelectrics | | | | | | |
| Potassium Dihydrogen Phosphate | | | | | | |
| Dielectric Constant | | | | | | |
| Tunneling Mode | | | | | | |

DD FORM 1 NOV 65 1473 (BACK)

S/N 0101-807-6821